



Università degli Studi Mediterranea di Reggio Calabria
Archivio Istituzionale dei prodotti della ricerca

Reconstructing the membrane detection of a 1D electrostatic-driven MEMS device by the shooting method: convergence analysis and ghost solutions identification

This is the peer reviewed version of the following article:

Original

Reconstructing the membrane detection of a 1D electrostatic-driven MEMS device by the shooting method: convergence analysis and ghost solutions identification / Angiulli, G; Jannelli, A; Morabito, Francesco Carlo; Versaci, M. - In: COMPUTATIONAL AND APPLIED MATHEMATICS. - ISSN 0101-8205. - 34:4(2018), pp. 133-146. [10.1007/s40314-017-0564-4]

Availability:

This version is available at: <https://hdl.handle.net/20.500.12318/1308> since: 2021-02-03T16:08:07Z

Published

DOI: <http://doi.org/10.1007/s40314-017-0564-4>

The final published version is available online at: <https://link.springer.com/article/10.1007/s40314-017->

Terms of use:

The terms and conditions for the reuse of this version of the manuscript are specified in the publishing policy. For all terms of use and more information see the publisher's website

Publisher copyright

This item was downloaded from IRIS Università Mediterranea di Reggio Calabria (<https://iris.unirc.it/>) When citing, please refer to the published version.

(Article begins on next page)

Reconstructing the membrane detection of a $1D$ electrostatic-driven MEMS device by the shooting method: convergence analysis and ghost solutions identification

**Giovanni Angiulli¹ · Alessandra Jannelli² ·
F. Carlo Morabito³ · Mario Versaci³**

Abstract In this paper, in the domain of $1D$ -membrane micro-electro-mechanical systems in which the electrostatic field is expressed in terms of geometric curvature of the membrane, we present a numerical approach based on shooting techniques to reconstruct the membrane profile in the device in steady-state case. In particular, starting from known results in literature about existence achieved by Schauder–Tychonoff’s fixed point approach and uniqueness, and focusing on two physical–mathematical parameters appropriately indicative of the applied voltage and electromechanical properties of the membrane, respectively, we will discuss what operation parameters (applied voltage, amplitude of electrostatic field) and for which electromechanical membrane characteristic of the device is permitted or not a convergence of the method with respect to analytical results. Finally, we will discuss in detail the detected ghost solutions.

Keywords MEMS · Electrostatic actuation · Boundary semi-linear elliptic problems · Boundary value problems · Shooting method

1 Introduction to the problem

In recent years, the ever-increasing demand for embedded engineering applications has driven research into low-cost, micro-nano-sized solutions where multi-functional actuators and sensors play a key role because they exploit the connection between the physical nature of the information and the need to make use of the machine language. In such a context, the interest of the scientific community for micro-electro-mechanical systems (MEMS) is growing more and more so that in a recent survey, these technologies have been considered among the most promising of the twenty-first century to support a new man-machine interface model that will be able to revolutionize the world of industry. MEMS technology, born in 1964 with the production of the first batch device (Nathanson et al. 1964), nowadays is an aspect of physical-mathematical multi-disciplines far from simple purely engineering application thanks to advanced modeling theories both in static and dynamic conditions. Although modern theories produce models that are true to reality, however, they do not allow for explicit solutions that must be satisfied with providing conditions that guarantee the existence, uniqueness and regularity of the solution. Therefore, under certain conditions, we seek for numerical solutions from implicit formulations. The Scientific Community, in the field of MEMS technologies, works extensively on two main fronts. The first, theoretically, is involved in the modeling of coupled problems: from topics relating to the modeling of magnetically actuated systems (Batra et al. 2007; Herrera-May et al. 2009), thermal-elastic systems (Huja and Husak 2001; Yang et al. 1997), electric-elastic systems (Bernstein et al. 2000; Pelesko and Chen 2003; Hassen et al. 2013) and micro-fluidics devices (Kaajakari 2009; Senturia 2001). The second, of applicative nature, operates in the field of technology transfer in different areas such as Bio-MEMS for medical diagnostics (Rezai et al. 2012; Castell 2005). In addition, in highly specialized physical-mathematical fields such as static-magneto-thermo-elastic problems modeling, for example, very good results have been produced both obtaining conditions guaranteeing the existence and uniqueness of the solution in particular functional spaces (Barba and Lorenzi 2013) and in the study of wave propagation in micro-domains (Payel and Kanoria 2009). In addition, with regard to transversely isotropic magneto-electro-elastic solid immersed in fluid, it has introduced a particular decoupling technique exploiting special potential functions (Selvamani and Pommusamy 2016). Recently, in the field of modeling of electrostatic actuators in both steady and dynamical cases, very interesting results on the existence, uniqueness and regularity have been carried out by means of near operator theory even if non-linear singularities take place (Cassani et al. 2009, 2014; Cassani and Tarsia 2016). There, the designed MEMS consists of two metal plates, one of which (the ground plate) is fixed and the other (top plate) is free to deform but clamped at boundary of a region $\Omega \in \mathbb{R}^N$, and it is subjected to a suitable voltage drop that deflects the top plate (located at $u = 0$) towards the ground plate ($u = 1$). The model that governs the deflection of the plate (Fig. 1), in the stationary case, is the following:

$$\begin{cases} \alpha \Delta^2 u = \left(\beta_1 \int_{\Omega} |\nabla u|^2 dx + \gamma \right) \Delta u + \frac{\lambda_1 f_1(x)}{(1-u)^{\sigma_1} \left(1 + \chi \int_{\Omega} \frac{dx}{(1-u)^{\sigma-1}} \right)} \\ u = \Delta u - du_{,v} = 0, \quad x \in \partial\Omega, \quad d \geq 0; \quad 0 < u < 1, \quad x \in \Omega \end{cases} \quad (1)$$

whose parameters shall have the meaning reported in Table 1 where a list of symbols exploited in this paper is displayed. An acceptable simplification is obtained by setting $\alpha = 1$, $\beta = \gamma = 0$ and $\sigma_1 = 2$, obtaining the following model:

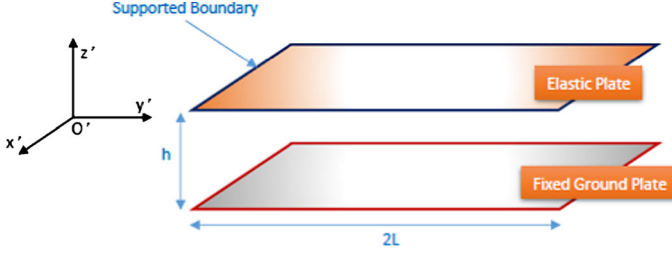


Fig. 1 A simplified representation of the device in which the elastic plate is at potential V and the fixed ground plate is at potential $V = 0$

Table 1 List of the exploited symbols

Symbol	Description
u	Deflection of the membrane
$\alpha, \beta_1, \gamma \in \mathbb{R}^+$	Mechanical rigidity, mechanical deformability and tangential mechanical tension of the deformable plate
ϕ, V	Electrostatic potential and applied electrical tension
$\chi \in \mathbb{R}^+$	Non-local dependence of ϕ on the solution
$\sigma_1 \geq 2, \epsilon_t$	Coulomb's exponent and dielectric strength of the membrane
$f_1(x)$	Electrical properties of the membrane (bounded function)
λ_1	Electrical voltage applied between the two plates
E, K	Magnitude of electrostatic field and curvature of the membrane
$\theta \in \mathbb{R}^+$	Proportionality coefficient between E^2 and $\lambda^2/(1-u(x))^2$
h, L_1	Distance between the two plates, semi-length of the device
σ, D	Mechanical tension and bending stiffness of the deformable plate
$\epsilon_0, \epsilon = h/(2L)$	Permittivity of free space, aspect ratio of the system
$\delta = D/((2L)^2\sigma)$	Relative importance of tension and rigidity
$\beta = \frac{\epsilon_0(2L_1)^2}{2h^3\sigma}$	Electro-mechanical properties of the membrane
β_1	Electro-mechanical properties of the material constituting the membrane in dimensionless conditions
d^*, α_1	Critical security distance, $1 - d^*$
$G(x, s), H, \overline{H}$	Green's function, $\sup u'(x) $ and $\sup H $
$\overline{\lambda^2} > 0$	Minimum voltage to apply to the MEMS device to win the mechanical inertia of the membrane

$$\begin{cases} \Delta^2 u(x) = \frac{\lambda_1 f_1(x)}{[1-u(x)]^2}; & 0 < u(x) < 1 \text{ in } \Omega, \\ u = \Delta u - du_\nu, & \text{on } \partial\Omega, \quad d \geq 0 \end{cases} \quad (2)$$

thoroughly studied in Cassani et al. (2009) which represents, in dimensionless constants, the limit case of zero ground plate thickness neglecting inertial effects and non-local effects too. Model (1), characterized by the presence of non-linearity that develops singularities, has been widely studied in which boundary conditions, assume an extremely delicate role. In particular, studies of existence with Steklov boundary conditions have been exploited to achieve Dirichlet and Navier boundary conditions when $d = 0$ or $d = \infty$ (see Cassani et al. 2011). In addition,

the problem of obtaining uniqueness conditions for (1) is still an open problem especially when $\sigma = 2$. The delicacy of fixing boundary conditions for (1) together with the difficulty of obtaining conditions of uniqueness makes the numerical study of (1) less interesting, especially if interested in highlighting the presence of numerical solutions that do not meet the analytical conditions of existence and uniqueness (ghost solutions). In this paper, for merely application interests, we focus our attention on a simplified 1D-membrane MEMS version of model (2) since the deformable plate has been replaced by a deformable membrane anchored along the edge of a plate so that the dimensionless model becomes (for details, see Pelesko and Bernstein 2003; Barba et al. 2017)¹:

$$\begin{cases} u'' = -\frac{\lambda_1}{(1-u)^2} \text{ in } \Omega \\ u(-L_1 = -1/2) = u(L_1 = 1/2) = 0. \end{cases} \quad (3)$$

In particular, this research has its starting point in the well-known analytical results of existence and uniqueness of the solution for (3) where the amplitude of the electric field E , that is $\lambda_1/(1-u)^2$, given that locally the electric field vector is orthogonal to the tangent line to the membrane, is proportional to the curvature K of the membrane whose profile is required to be C^{22} Barba et al. (2017). The problem, thus, reformulated is depending on the product of two parameters, θ and λ^2 , significant of the applied voltage V and electromechanical properties of the membrane, respectively. In this paper, after having properly rewritten the condition that guarantees the existence of the solution, by numerical shooting techniques, we wonder:

1. for which values of $\theta\lambda^2$ the convergence of the numerical procedure is allowed/not allowed;
2. $\theta\lambda^2$ values under convergence that do not respect both analytical existence and uniqueness conditions (ghost solutions);
3. electromechanical characteristics of the membrane and voltage V and electrical field amplitude E (operation parameters) not allowed in convergence;
4. electromechanical characteristics of the membrane and operation parameters related to the ghost solutions;
5. electromechanical characteristics of the membrane and operation parameters in condition of convergence that respect the analytical existence and uniqueness conditions.

The shooting method works by considering the boundary conditions as a multivariate function of initial conditions at some point, reducing the boundary value problem to find the initial conditions that give a root. The advantage of the shooting method is that it takes advantage of the speed and adaptivity of the numerical methods usually used in solving the initial value problems. The disadvantage of the method is that it is not as robust as finite difference or collocation methods: some initial value problems with growing modes are inherently unstable even though the BVP itself may be quite well posed and stable. The paper is organized as follows. Section 2 describes in details some backgrounds useful for implementing the mathematical formulation of the model in terms of curvature K of the membrane. In the following, Sect. 3 recalls a well-known result of the existence and uniqueness of the solution for it and rewrite appropriately the condition of existence. Section 4, then, describes the proposed numerical approach based on shooting techniques applied to the model under study providing useful convergence results in view of the purposes and respecting the conditions of existence and uniqueness above mentioned (Sect. 5). Finally, Sect. 6 outlines some significant conclusions and opening up new developments.

¹ – is due to the opposite orientation of the vertical axis.

² When the deformation takes places, membrane profile, point-to-point slope and curvature are continuous functions.

2 Some useful backgrounds

The approach followed in this study comes from Barba et al. (2017) in which in \tilde{P} the amplitude of the electrostatic field E is considered to be proportional to the curvature of the membrane taking into account that, locally, the vector electrostatic field is orthogonal to the tangent straight to the membrane. In more detail, taking into account that $\lambda_1 = \lambda^2 = \epsilon_0 V^2 (2L)^2 / 2h^3 \sigma = \beta V^2$ so that $\lambda^2 / (1 - u)^2$ is proportional to the square of the magnitude of E , \tilde{P} can be written as the following problem \tilde{P} :

$$\tilde{P} : \begin{cases} -u'' = \theta E^2 & \text{in } \Omega \subseteq \mathbb{R}^n \\ \theta \in \mathbb{R}^+; \quad u(-L_1) = u(L_1) = 0. \end{cases} \quad (4)$$

Obviously, θ should be depending on x but, for obvious physical reasons, it is continue function over $[-L_1, L_1]$ so that it is a bounded function and, therefore, it is always lower than a positive real θ . Indicating by $K(x, u(x))$ the curvature of the deformed membrane and by $\mu(x, u(x))$ the proportionality function between E and K , the following expression holds³:

$$E(x) = \mu(x, u(x))K(x, u(x)) \quad (5)$$

so that (4) can be written as:

$$\tilde{P} : \begin{cases} -u'' = \theta \mu^2(x, u(x))K^2(x, u(x)) = \theta \lambda^2 \frac{K^2(x, u(x))}{(1 - u(x) - d^*)^2} & \text{in } \Omega \subseteq \mathbb{R}^n \\ u(-L_1) = u(L_1) = 0; \quad \theta \in \mathbb{R}^+; \quad 0 < u(x) < \alpha_1 = 1 - d^*, \end{cases} \quad (6)$$

where d^* is the critical security distance to ensure that the deflection of the membrane does not touch the top plate of the device so that $\mu(x, u(x), \lambda) = \lambda / (1 - u(x) - d^*)$ with $\mu(x, u(x)) \in C^0(A)$, $A = [-L_1, L_1] \times [0, 1)$. Finally, expressing the curvature K by the well-known 1D expression $K(x, u(x)) = |u''(x)| / \sqrt{(1 + |u'(x)|^2)^3}$, (6) can be written as:

$$\tilde{P} : \begin{cases} u''(x) = -\frac{1}{\theta \lambda^2} (1 + (u'(x))^2)^3 (\alpha_1 - u(x))^2 & \text{in } \Omega = (-L_1, L_1) \\ u(-L_1) = u(L_1) = 0 \text{ on } \partial\Omega; \quad \theta \in \mathbb{R}^+; \quad 0 < u(x) < \alpha_1 = 1 - d^*, \end{cases} \quad (7)$$

where $\frac{1}{\theta \lambda^2} (1 + (u'(x))^2)^3 (\alpha - u(x))^2 \in C^0(\overline{\Omega} \times \mathbb{R} \times \mathbb{R})$ and $u \in C^2([-L_1, L_1])$ ⁴ and $\mu = \mu(x, u(x), \lambda) \in C^0([-L_1, L_1]) \times \mathbb{R}$. However, a final clarification is required. Problem (7) apparently there is no singularity highlighted by (3) when $u = \alpha_1$. But observing (7), if $u(x) = \alpha_1$ we would get $u''(x) = 0$ obtaining a linear profile of the membrane with $E = 0$ (for details, see Barba et al. 2017).

Some further physical considerations Product $\theta \lambda^2$ in (7) immediately appears to be of fundamental importance for both physically meaning and convergence of the applicable numerical methods. From a physical point of view, θ is the parameter representing the proportionality between E^2 and $\lambda^2 / (1 - u)^2$, (and, therefore, the applied voltage) while $\lambda^2 = \epsilon_0 V^2 (2L)^2 / 2h^3 \sigma = \beta V^2$ is the parameter that takes into account, in addition to the applied voltage, of the electro-mechanical properties (β) of the material constituting the

³ Functional dependency on x and $u(x)$ for both K and μ has been highlighted by a study carried out on well-known hemispherical benchmark in literature (Voltmer 2007).

⁴ Plausible condition because the membrane does not allow tears and its slope varies with continuity.

membrane.⁵ In other words, the following chain of equality holds:

$$\theta E^2 = \frac{\lambda^2}{(1-u)^2} = \frac{\epsilon_0 V^2 (2L)^2}{2h^3 \sigma (1-u)^2} = \frac{\beta V^2}{(1-u)^2}. \quad (8)$$

3 Rewriting of some important analytical results for problem \tilde{P}

As (7) does not allow to obtain the deflection of the membrane $u(x)$ explicitly, we report a result, known in literature, of existence and uniqueness of the solution (Barba et al. 2017). Specifically, (7), by differentiation, can be transformed in the integral equation $u(x) = \int_{-L_1}^{L_1} G(x, s) \left[\frac{(1+(u'(s))^2)^3}{\beta \mu^2(s, u(s), \lambda)} \right] ds$ where $G(x, s)$ is a suitable Green's function.⁶ Considering also the equation $T(u) = w$ with $u \in P_1$ where $P_1 = \{C_0^1[-L_1, L_1] : 0 < u(x) < \alpha_1, |u'(x)| < H < +\infty\}$ and $H = \sup|u'(x)|$ for each eligible profile u ; exploiting the Schauder–Tychonoff fixed point theorem applied to the operator $T(u) = w$ from P to P with $P = \{C_0^2[-L_1, L_1] : 0 < u(x) < \alpha_1, |u'(x)| < H < +\infty\}$ it is proved the existence of at least one solution for $T(u) = w$ when

$$1 + H^6 < \frac{H\theta\bar{\lambda}^2}{4\alpha_1 L_1}, \quad (10)$$

where $\bar{\lambda}^2 > 0$ represents the minimum voltage, depending on the material constituting the membrane to apply to the MEMS device to win the mechanical inertia of the membrane:

$$\bar{\lambda}^2 < \lambda^2 < \sup(\lambda^2). \quad (11)$$

In fact, condition (10) reported in Barba et al. (2017) assumes the form

$$1 + H^6 < \frac{H\beta\bar{\lambda}^2}{2\alpha_1 L_1} \quad (12)$$

but, taking into account the (8), we can write⁷

$$1 + H^6 < \frac{H\beta\bar{\lambda}^2}{4\alpha_1 L_1} = \frac{H}{4\alpha_1 L_1} \frac{E^2(1-u)^2\theta\bar{\lambda}^2}{V^2} = \frac{H}{4\alpha_1 L_1} \theta\bar{\lambda}^2 \quad (13)$$

so (10) applies. Further, from (10) it is possible to write $H < \sqrt[6]{\frac{\theta\bar{\lambda}^2}{4L_1^2} - 1}$ whose numerical verifications had pointed out that necessary

$$\bar{H} = \sup|H| = 99 \quad (14)$$

corresponding to an angle of 88.92° in dimensionless conditions fully compatible with the experimental experience (for details, see Barba et al. 2017). With respect to the condition (10), to obtain the deflection of the membrane, it is obviously necessary a numerical approach.

⁵ For $\sigma \rightarrow 0$, β assumes high values indicating less membrane deformation capacity.

⁶ In our case, the exploited Green's function is Bayley et al. (1968)

$$G(x, s) = \begin{cases} \frac{(s+L_1)(L_1-x)}{2L_1} & -L_1 \leq s \leq x \\ \frac{(L_1-s)(x+L_1)}{2L_1} & x \leq s \leq L_1. \end{cases} \quad (9)$$

⁷ Given that $(1-u)^2 < 1$ and E^2/V^2 is the distance between the plates ($= 1$).

With regard to the uniqueness of the solution for (7), the following results are worth (Barba et al. 2017):

Theorem 1 $\forall H > 0$ the solution of the Problem \tilde{P} is unique. In addition, the following properties hold:

1. $\forall x \in [-L_1, L_1]$, $|u'(x)| \leq |u'(L)| = |u'(-L)|$;
2. u is symmetric with respect to the origin;
3. $u \in C^\infty([-L_1, L_1])$;
4. u is analytical.

highlighting that (7) accepts a unique solution.

4 The proposed numerical approach

In this section, we present the numerical method used to solve the mathematical model \tilde{P} . As a first step we rewrite it as a first-order system

$$\begin{cases} u_1' = u_2 \\ u_2' = -\frac{1}{\theta\lambda^2}(1 + u_2^2)^3(\alpha_1 - u_1)^2 \\ u_1(-L) = 0 & u_1(L) = 0 \end{cases} \quad (15)$$

by setting

$$\begin{aligned} u_1(x) &= u(x), \\ u_2(x) &= \frac{du_1}{dx}(x) = \frac{du}{dx}(x). \end{aligned}$$

To solve the resulting problem, we apply a classical shooting method. The BVP (15) will turn into an IVP if we replace the boundary condition of the solution $u_1(L)$ at $x = L$ with the following initial condition

$$u_2(-L) = \eta, \quad (16)$$

where η is some number. Then we can integrate the resulting problem as an initial value problem by a suitable numerical method and obtain the value of its solution $u_1(L)$ at $x = L$. If $u_1(L) = 0$, then we have solved the BVP. In this way it defines, implicitly, a non-linear equation $F(\eta) = u_1(L; \eta) = 0$. The idea is now to find the right value of η iteratively by a root-finder method. The simplest such a method is the secant method. It is known that the secant method is convergent provided that the initial iterates are sufficiently close to the root, and that the order of the convergence is super-linear, that is equal to $(1 + \sqrt{5})/2$. By starting with suitable values of η_0 and η_1 , the root-finder method is used to define a sequence η_k for $k = 2, 3, \dots$. At each iteration the value η_k is obtained by solving the IVP numerically. Suitable termination criteria have to be used to verify whether $\eta_k \rightarrow \eta$ as $k \rightarrow \infty$. The numerical results reported in the next section are obtained by setting $\eta_0 = 1.1$ and $\eta_1 = 1.2$ as initial guess, the classical convergence criteria are used with a tolerance 10^{-12} . The numerical solutions of the initial value problem are obtained by the *ODE23* solver, from the MATLAB ODE suite written by Shampine and Reichelt (2011), with the accuracy and adaptivity parameters defined by default. Note that it is possible to apply the shooting method also implementing the iterative Newton's method. By the computational complexity point of view, the method requires the evaluation of the Jacobian, that generally

can be computed using the finite differences. Because the sensitivity of solutions of an initial value problem to its initial conditions may be too much to get reasonably accurate derivative values, it is advantageous to compute the Jacobian as a solution to ODEs. This requires a more complex numerical treatment of the model because a system with a doubled dimension has to be solved. Then, we have found that the secant method is particularly suitable in this context. In addition, by our numerical experiments, more restrictive convergence conditions have pushed us to exclude the Newton method. A comparison with the numerical results obtained with a relaxation method has highlighted a high computational cost of the latter compared to the proposed shooting method. The tests carried out showed that the convergence of the numerical method and the accuracy of the results are obtained with a large number of grid points. The considerably high computational cost of the relaxation method led the authors to exclude it (Fazio and Jannelli 2014, 2017; Keller 1974).

5 Convergence conditions and numerical results of interest

To test the proposed numerical methodology (implemented on Intel Core 2 CPU 1.47 GHz using MatLab R2009a), a large number of tests have been carried out with $d^* = 0.0001$ to evaluate the range of $\theta\lambda^2$ values that ensures convergence⁸ in compliance with the conditions (10), (11) and (14). In addition, from this range, a sub-range representing the ghost solutions of the problem under study was extracted. The choice to fix $d^* = 0.0001$ was dictated by the fact that it represents a tiny fraction of the distance $h = 1$ enough to ensure that $u(x) < 1$. The following remarks describe in detail the main results obtained with particular reference to the possible engineering applications and membrane materials that can be used in convergence conditions.

Remark 1 On the convergence/non-convergence of the numerical procedure. In the event that $\theta\lambda^2 \in [0.63, +\infty)$ the convergence is guaranteed, pointing to $(\theta\lambda^2)_{\text{conv}} = [0.63, +\infty)$, we can write:

$$\inf\{(\theta\lambda^2)_{\text{conv}}\} = \min\{(\theta\lambda^2)_{\text{conv}}\} = 0.63. \quad (17)$$

Obviously, if $\theta\lambda^2 \in [0, 0.63)$ the procedure does not always converge.

Remark 2 On checking the analytical condition (14). As shown in Table 2 and in Fig. 2, $\forall\theta\lambda^2 \in (\theta\lambda^2)_{\text{conv}}$ the values of $\sup\{u'(x)\}$ numerically achieved are all smaller than 99 as required by (14) also highlighting that, as $\theta\lambda^2$ increases, the membrane profile tends to flatten. In addition, these values show a good symmetry of the membrane profile with respect to the axis $x = 0$ completely adhering to the fact that the applied tension urges the membrane to rise symmetrically with respect to the same axis. It is worth noting that the value 99 is considerably higher than the $|u'(x)|$ values numerically achieved. This is due to the fact that to obtain the (14), in Barba et al. (2017) the authors have constructed a sequence of a lot inequalities that gradually emerged in the calculations. Such increased values (constant values) were extracted from the integrals that were formed and which were easily calculated. The number of inequalities was quite high so that the value equal to 99 is surely excessive but analytically correct. At any case, this value respects the experimentation that also allows high membrane deformations. The numerical results reported are obtained with an average number of iterations equal to 10.

⁸ And, for complementarity, the range of values that does not ensure convergence.

Table 2 Some typical values of $\max(u'(x))$ when $\theta\lambda^2 \in (\theta\lambda^2)_{\text{conv}}$ detectable at the end of the membrane

$\theta\lambda^2 \in (\theta\lambda^2)_{\text{conv}}$	$u'(-0.5)$	$u'(0.5)$	$\theta\lambda^2 \in (\theta\lambda^2)_{\text{conv}}$	$u'(-0.5)$	$u'(0.5)$
<i>0.63</i>	<i>4.131</i>	<i>-4.131</i>	1.4	0.358	-0.358
<i>0.64</i>	<i>2.035</i>	<i>-2.035</i>	1.6	0.309	-0.309
$(\theta\lambda^2)_1 = 0.642$	1.964	-1.964	2.0	0.244	-0.244
0.65	1.674	-1.674	2.2	0.221	-0.221
0.7	1.114	-1.114	2.4	0.202	-0.202
0.72	1.015	-1.015	2.6	0.187	-0.187
0.73	0.975	-0.975	2.8	0.173	-0.173
0.74	0.939	-0.939	3	0.1621	-0.162
0.76	0.879	-0.879	3.2	0.1520	-0.152
0.78	0.828	-0.828	3.4	0.1431	-0.143
0.8	0.785	-0.785	3.6	0.1353	-0.135
1	0.544	-0.544	3.8	0.1282	-0.128
1.2	0.429	-0.429	4	0.1218	-0.121

In italics, $\theta\lambda^2$ values that give us the ghost solutions. $(\theta\lambda^2)_1 = 0.642$ (in bold) represents the $\sup(\theta\lambda^2)$ of such solutions (see Remark 4)

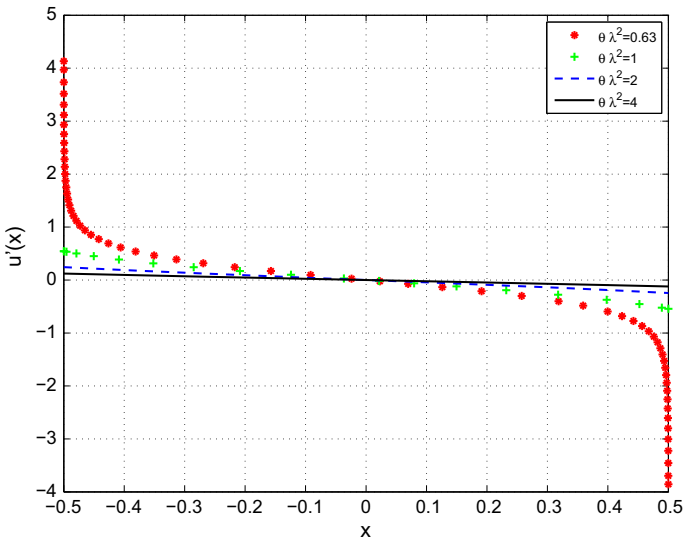


Fig. 2 $H = \sup\{u'(x)\}$ when $\theta\lambda^2 \in (\theta\lambda^2)_{\text{conv}}$: in addition to the obvious symmetry over the device's mid-range, the higher is the value of $\theta\lambda^2$, the lower is the membrane deflection

Remark 3 On the confirmation of the condition (10) and finding of the ghost solutions. Bearing in mind the condition (10) that guarantees the existence of the solution to the problem⁹ and the (11), we observe that

$$\bar{\lambda}^{-2} < \lambda^2 < \sup\{\lambda^2\} \tag{18}$$

⁹ Let us remember that the uniqueness of the solution for problem (7) is always guaranteed.

and then, for $\theta \neq 0$, the following relation applies

$$\theta \bar{\lambda}^2 < \theta \lambda^2 < \sup\{\theta \lambda^2\} \quad (19)$$

so that it is permissible to write

$$1 + H^6 < \frac{H\theta \bar{\lambda}^2}{4\alpha_1 L_1} < \frac{H\theta \lambda^2}{4\alpha_1 L_1} = \frac{H\theta \lambda^2}{2\alpha_1}. \quad (20)$$

exclusively referred for $H = 99$. Then, taking into account that

$$\begin{aligned} H &= \sup\{|u'(x)|\} = 99; \quad \inf\{\lambda^2\} = \bar{\lambda}^2; \quad \alpha = 1 - d^* \\ \lambda^2 &= \theta V^2; \quad \theta \geq 10^{12} \end{aligned} \quad (21)$$

from (20) we can write:

$$1 + 99^6 < \frac{99\theta^2 V^2}{2\alpha} \quad (22)$$

and since $1 + 99^6 \simeq 99^6$, (22) assumes the form:

$$99^6 < \frac{99\theta^2 V^2}{2\alpha} \quad (23)$$

from which, taking into account (21), we can write:

$$V > \sqrt{2 \frac{99^5}{\theta^2} (1 - d^*)} = 1.3791 \cdot 10^{-7}. \quad (24)$$

Inequality (24), with the usual values of θ , is an extremely small value and again, considering condition (21), $\theta \geq 10^{12}$ so that condition (24) can be exploited in the following as the $\sup\{\inf\{V\}\}$ to the benefit of security. Let us now point to H_j the value of $\max|u'(x)|$ for the j -th profile achieved in condition of convergence, where $j \in J \subset \mathbb{N}$. As $H_j < H$, it is permissible to write

$$1 + H_j^6 < 1 + H^6 \quad (25)$$

and, taking into account (20), we can write:

$$1 + H_j^6 < \frac{H\theta \lambda^2}{2\alpha}. \quad (26)$$

Now, to ensure convergence, $\theta \lambda^2 \geq 0.63$ so that (26) assumes the following form:

$$1 + H_j^6 < \frac{99 \cdot 0.63}{2\alpha} = \frac{31.185}{1 - d^*} \quad (27)$$

and again

$$H_j < \sqrt[6]{\frac{31.185}{1 - d^*} - 1} \quad (28)$$

from which, considering d^* small enough, we can write:

$$H_j < \sqrt[6]{30.185} = 1.7645. \quad (29)$$

In other words, convergence is guaranteed when the maximum slope of the membrane is less than 1.7645. Obviously, varying $\theta \lambda^2$ (and in particular increasing $\theta \lambda^2$ to ensure convergence) (28) can be written as:

$$H_j < \sqrt[6]{\frac{49.5\theta \lambda^2}{1 - d^*} - 1} \quad (30)$$

whose performance, when $d^* = 0.0001$, is shown in Fig. 3a, where the blue curve represents the (30) in terms of equality (so the permissible values of H_j must lie below this curve) while the green line identifies the values of $H_{\text{numerical}}$ carried out numerically. Finally, the red vertical line identifies $\min\{(\theta\lambda^2)_{\text{conv}}\}$ from which numerical convergence is guaranteed. An enlargement of Fig. 3a is displayed in Fig. 3b from which one can see the intersection between the blue curve (H_j vs $\theta\lambda^2$) and the green curve ($H_{\text{numerical}}$ vs $\theta\lambda^2$) highlighted by the black vertical line. If $\theta\lambda^2 \in [\min\{(\theta\lambda^2)_{\text{conv}}\} (\theta\lambda^2)_1)$ the procedure provides solutions numerically acceptable but do not meet the condition (10), so that they represent the ghost solutions (in Fig. 3b, the area between the red and black vertical lines). It is worth pointing out that (30) can not be exploited to determine which operation parameters (pairs $(V, \sup\{E^2\})$) and for which devices the converge of the procedure is permissible with respect to the numerical results since, from it, $\theta\lambda^2$ would be a function of H_j that can not be *a priori* quantified. The following remarks solve the problem following an alternative approach in which H_j is not involved.

Remark 4 Some physical–analytical confirmations. Figure 4 shows typical membrane profile performance ($u(x)$) for different $\theta\lambda^2 \in (\theta\lambda^2)_{\text{conv}}$, confirming the increase in deflection to the decrease of $\theta\lambda^2$. It agrees both analytically and physically with the analytical model (7). In fact, $\theta\lambda^2$, appearing at the denominator of the second member in (7), significantly affects the concavity of the membrane (proportional to $u''(x)$), the only term available to the first member in (7), so by increasing $\theta\lambda^2$ values the concavity of the membrane is reduced. On the other hand, as $\theta\lambda^2 \propto \beta^2 V^2$, and β is much bigger than V , $\theta\lambda^2$ increase implies that: 1) if we set V^{210} : β increases but the applied voltage is insufficient to deform the membrane, resulting in a decrease in the concavity of the profile $u(x)$; 2) if we set β^{11} : the increase in V can not deform the membrane, so even in this case, concavity of $u(x)$ decreases.

Remark 5 Electromechanical characteristics of the membrane and operation parameters that are not allowed in convergence. Multiplying (8) by λ^2 and taking into account that $(1-u)^2 < 1$, $E^2 < \sup\{E^2\}$, $\beta_1 = \epsilon_0/2\sigma$ e $\lambda^2 = \beta_1 V^2$, it is permissible to write:

$$\theta\lambda^2 E^2 = \frac{\beta_1 V^2 \lambda^2}{(1-u)^2} = \frac{\beta_1^2 V^4}{(1-u)^2} \quad (31)$$

from which

$$\theta\lambda^2 = \frac{\epsilon_0^2 V^4}{4\sigma^2(1-u)^2 E^2} > \frac{\epsilon_0^2 V^4}{4\sigma^2 \sup\{E^2\}}. \quad (32)$$

As in non-convergence conditions $\theta\lambda^2 < 0.63$,¹² the Electromechanical characteristics of the membrane (parameter σ) and operation parameters (pair $(V, \sup\{E^2\})$) that meet the following inequality:

$$\frac{\epsilon_0^2 V^4}{4\sigma^2 \sup\{E^2\}} < 0.63. \quad (33)$$

In particular, for a particular pair $(V^*, \sup\{E^{*2}\})$ and taking into account the (24), only Electromechanical characteristics of the membrane whose σ

$$\begin{cases} \sigma > \frac{\epsilon_0 V^{*2}}{2\sqrt{0.63 \sup\{E^2\}}} \\ V^* > 1.3791 \cdot 10^{-7} \end{cases} \quad (34)$$

¹⁰ In other words we are considering a particular engineering application.

¹¹ That is, we choose the material constituting the membrane.

¹² In the sense that convergence is not guaranteed.

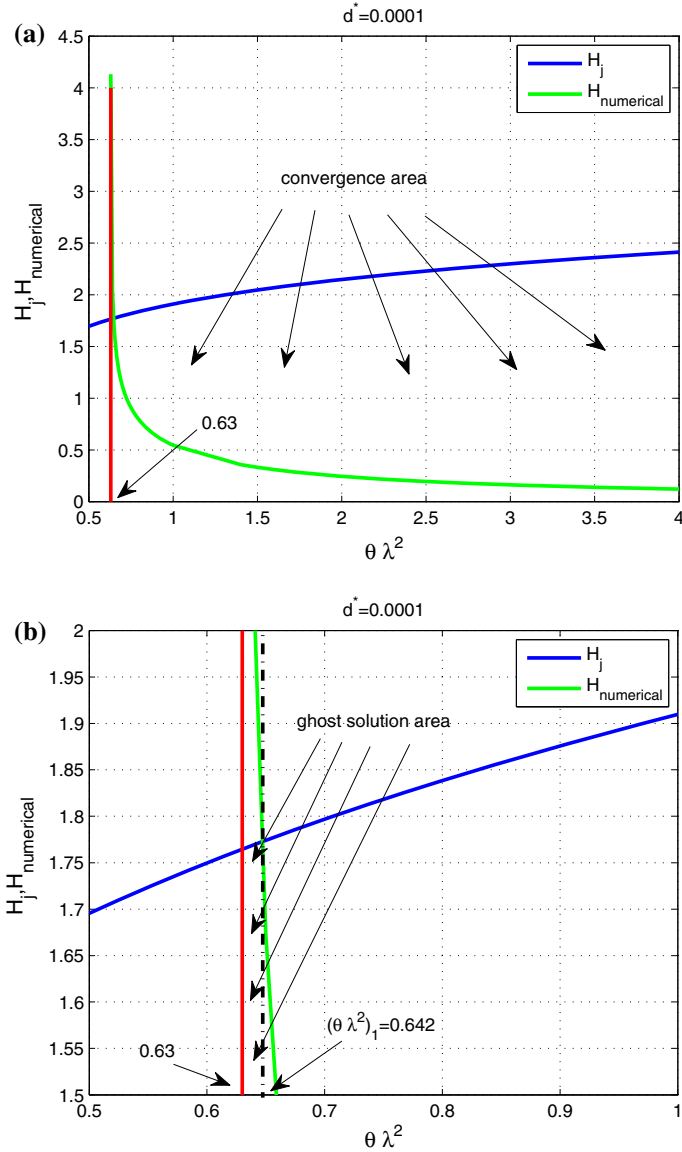


Fig. 3 H_j and $H_{\text{numerical}}$ depending on $\theta \lambda^2$ with $d^* = 0.0001$: if $\theta \lambda^2 \in (\theta \lambda^2)_{\text{conv}}$ the convergence is guaranteed (a); if $\min\{(\theta \lambda^2)_{\text{conv}}\} \leq \theta \lambda^2 < (\theta \lambda^2)_1 = 0.642$, even if the condition of convergence is verified, (10) is not satisfied (ghost solutions) (b)

must be avoided. Conversely, considering again the condition (24), the membrane with a fixed σ^* can not be used requiring

$$\begin{cases} \frac{(1.3791 \cdot 10^{-7})^4}{\sup\{E^2\}} \leq \frac{V^4}{\sup\{E^2\}} < \frac{2.52\sigma^2}{\epsilon_0^2} \\ V > 1.3791 \cdot 10^{-7}. \end{cases} \quad (35)$$

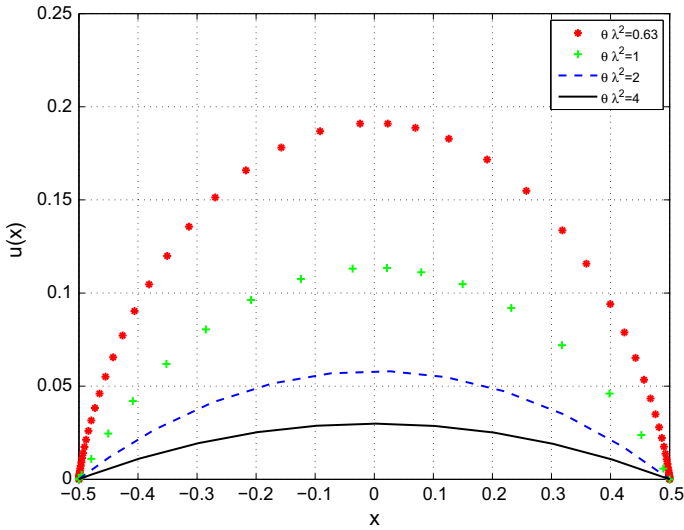


Fig. 4 $u(x)$ profiles of the membrane for different $\theta\lambda^2$ values. Deflection increases as these values decrease

Remark 6 Electromechanical characteristics of the membrane and operation parameters related to the ghost solutions. Obviously, all membranes and operation parameters satisfying the following inequality

$$0.63 \leq \frac{\epsilon_0^2 V^4}{4\sigma^2 \sup\{E^2\}} < 0.642 \tag{36}$$

ensure the presence of ghost solution. In particular, for a particular pair $(V^*, \sup\{E^{*2}\})$, membranes satisfying the following sequence of inequalities

$$\begin{cases} \frac{2.52\sigma^2}{\epsilon_0^2} \leq \frac{V^{*4}}{\sup\{E^{*2}\}} < \frac{2.568\sigma^2}{\epsilon_0^2} \\ V^* > 1.3791 \cdot 10^{-7} \end{cases} \tag{37}$$

determine ghost solutions which also occur when, fixed a particular membrane (σ^*) and taking into account the (24), it will be exploited for operation parameters satisfying the following chain of inequalities:

$$\begin{cases} \frac{2.52\sup\{E^2\}}{V^4} \leq \frac{\epsilon_0^2}{\sigma^{*2}} < \frac{2.568\sup\{E^2\}}{V^4} \\ V > 1.3791 \cdot 10^{-7}. \end{cases} \tag{38}$$

Remark 7 Electromechanical characteristics of the membrane and operation parameters in convergence area that respect the condition (10). Finally, if operation parameters and Electromechanical characteristics of the membrane satisfying the following inequality

$$\frac{\epsilon_0^2 V^4}{4\sigma^2 \sup\{E^2\}} \geq 0.642 \tag{39}$$

we are working in convergence area and respecting the condition of existence and uniqueness of problem under study. Setting a particular pair $(V^*, \sup\{E^{*2}\})$ and considering condition (24), the membranes whose σ satisfies

$$\begin{cases} \frac{\epsilon_0^2}{\sigma^2} \geq 2.568 \frac{\sup\{E^{*2}\}}{V^{*4}} \\ V^* > 1.3791 \cdot 10^{-7} \end{cases} \quad (40)$$

are compatible. In addition, if one chooses a particular membrane (σ^*), convergence existence and uniqueness of the solution are ensured for all parameters for which

$$\begin{cases} \frac{\epsilon_0^2}{\sigma^{*2}} \geq 2.568 \frac{\sup\{E^2\}}{V^4} \\ V > 1.3791 \cdot 10^{-7}. \end{cases} \quad (41)$$

6 Conclusion and perspectives

In this work, a numerical approach has been presented for the reconstruction of the membrane profile $u(x)$ in 1D MEMS devices in which the applied voltage V produces an electrostatic field \mathbf{E} whose direction is, locally, orthogonal to the surface of the membrane. The starting point of the research is represented by a mathematical model of the MEMS device where $|\mathbf{E}|$ is considered proportional to the curvature of the membrane and characterized by the impossibility of detaching the solution analytically but its conditions of existence and uniqueness for the solution are known. Here, by first rewriting appropriately the condition of existence of the solution, an equivalent problem was tackled and solved by a numerical shooting approach together with method of secants and the MatLab solver for ODE. In this way, we have taken the advantage of the speed and adaptivity of the ODE solver. The tests showed that the convergence of the numerical method depended on $\theta\lambda^2$ product, that is on physical parameters related to the operation parameters (pair $(V^*, \sup\{E^2\})$) and the electromechanical characteristics of the membrane (parameter σ). In particular, this study has highlighted the $\theta\lambda^2$ value, indicated by $\min\{(\theta\lambda^2)_{\text{conv}}\} = 0.63$, from which the convergence of the numerical method is guaranteed. Complementary, $\theta\lambda^2$ values lower than $\min\{(\theta\lambda^2)_{\text{conv}}\}$ ensure the non-convergence of the procedure. A special $\theta\lambda^2$ value, $(\theta\lambda^2)_1 = 0.642$, has also been identified beyond which the method, in addition to being convergent, avoids the presence of ghost solutions as the obtained numerical solutions surely satisfy the condition of existence and uniqueness of the equivalent analytic problem. In addition, in convergence (including ghost solutions)/unreliable convergence conditions, possible combinations of Electromechanical characteristics of the membrane and operation parameters have been obtained. Considering the regularity of the obtained solutions in conjunction with the adherence of analytical results to well-established experimental facts, the obtained results can be considered more than encouraging. However, more sophisticated of the curvature K could provide better results but with higher regularities required for the solution. Obviously, this study has exploited the numerical approach of a simplified 1D model of MEMS membrane devices in which E is considered proportional to K . Then, it is desirable to study more sophisticated 1D and 2D analytical models to find out conditions of existence and uniqueness of the solutions and, numerically, to evaluate the engineering areas of applicability of such devices.

References

- Bayley PB, Shampine LF, Waltman PE (1968) Nonlinear two point boundary value problems. Academic, New York
- Batra RC, Porfiri M, Spillo D (2007) Review of modeling electrostatically actuated microelectromechanical systems. J Microelectromech Syst 6:23–31

- Bernstein D, Guidotti P, Pelesko J (2000) Analytical and numerical analysis of electrostatically actuated MEMS devices. *Proc MSM* 2000:489–492
- Cassani D, d'O M, Ghossoub N (2009) On a fourth order elliptic problem with a singular nonlinearity. *Nonlinear Stud* 9:189–292
- Cassani D, Fattorusso L, Tarsia A (2011) Global existence for nonlocal MEMS. *Nonlinear Anal* 74:5722–5726
- Cassani D, Tarsia A (2016) Periodic solutions to nonlocal MEMS equations. *Discret Contin Dyn Syst Series* 9(3):631–642
- Cassani D, Fattorusso L, Tarsia A (2014) Nonlocal dynamic problems with singular nonlinearities and application to MEMS. *Progress Nonlinear Differ Equ Appl* 85:185–206
- Castell R (2005) Modeling the electrostatic actuation of MEMS. State of the art 2005, MEMS for biomedical applications
- Payel P Das, Kanoria M (2009) Magneto-thermo-elastic waves in an infinite perfectly conducting elastic solid with energy dissipation. *Appl Math Mech* 30(2):221–228
- Di Barba P, Lorenzi A (2013) A magneto-thermo-elastic identification problem with a moving boundary in a micro-device. *Milan J Math* 81(2):347–383
- Di Barba P, Fattorusso L, Versaci M (2017) Electrostatic field in terms of geometric curvature in membrane MEMS devices. *Commun Appl Ind Math* 8(1):165–184. <https://doi.org/10.1515/caim-2017-0009>
- Fazio R, Jannelli A (2014) Finite difference schemes on quasi-uniform grids for BVPs on infinite intervals. *J Comput Appl Math* 269:14–23
- Fazio R, Jannelli A (2017) BVPs on infinite intervals: a test problem, a nonstandard finite difference scheme and a posteriori error estimator. *Math Methods Appl Sci* 40:6285–6294. <https://doi.org/10.1002/mma.4456>
- Hassen MO, Hawa MA, Alqahtani HM (2013) Modeling the electrostatic deflection of a MEMS multilayers based actuator. *Math Probl Eng* 2013:1–12
- Herrera-May A, Aguilera-Cortes L, Garcia-Ramirez P (2009) Resonant magnetic field sensors based on MEMS technology. *Sensors* 9(10):4691–1695
- Huja M, Husak M (2001) Thermal microactuators for optical purpose. In: Proceedings of international conference on information technology: coding and computing, IEEE, Las Vegas, 2–4 Apr 2001. <https://doi.org/10.1109/ITCC.2001.918779>
- Kaajakari V (2009) MEMS tutorial: nonlinearity in micromechanical resonators. *MEMS Mater* 1–7
- Keller HB (1974) Accurate difference methods for nonlinear two-point boundary value problems. *SIAM J Numer Anal* 11:305–320
- Nathanson HC, Newell WE, Wickstrom RA, Lewis JR (1964) The resonant gate transistor. *IEEE Trans Electr Dev* 14:117–133
- Pelesko JA, Chen XY (2003) Electrostatic deflections of circular elastic membranes. *J Electrostat* 57(1):1–12
- Pelesko JA, Bernstein DH (2003) Modeling MEMS and NEMS. CRC Press Company, Boca Raton
- Rezai P, Wu W, Selvaganapathy P (2012) MEMS for biomedical applications. *MEMS Biomed Appl* 4:3–45
- Selvamani R, Pommusamy P (2016) Wave propagation in a transversely isotropic magneto-electro-elastic solid bar immersed in an inviscid fluid. *J Egypt Math Soc* 24:92–99
- Senturia SD (2001) Microsystem design. Kluwer Academic Publisher, Boston
- Shampine LF, Reichelt MW (2011) The MATLAB ODE suite. *SIAM J Sci Comput* 18:1–22
- Voltmer D (2017) Fundamentals of electromagnetics 1: internal behavior of lumped elements. In: Synthesis lectures on computational electromagnetics
- Yang X, Tai YC, Ho CM (1997) Micro bellow actuators. *Transducers* 97:45–58